Journal of Computational Physics, 231 (1), 2012, pp. 173–189.

Positivity-preserving High-resolution Schemes for Systems of Conservation Laws

Bernard Parent*

A new class of flux-limited schemes for systems of conservation laws is presented that is both high-resolution and positivity-preserving. The schemes are obtained by extending the Steger-Warming method to second-order accuracy through the use of component-wise TVD flux limiters while ensuring that the coefficients of the discretization equation are positive. A coefficient is considered positive if it has all-positive eigenvalues and has the same eigenvectors as those of the convective flux Jacobian evaluated at the corresponding node. For certain systems of conservation laws, such as the Euler equations for instance, this condition is sufficient to guarantee positivity-preservation. The method proposed is advantaged over previous positivity-preserving flux-limited schemes by being capable to capture with high resolution all wave types (including contact discontinuities, shocks, and expansion fans). Several test cases are considered in which the Euler equations in generalized curvilinear coordinates are solved in 1D, 2D, and 3D. The test cases confirm that the proposed schemes are positivity-preserving while not being significantly more dissipative than the conventional TVD methods. The schemes are written in general matrix form and can be used to solve other systems of conservation laws, as long as they are homogeneous of degree one.

1. Introduction

POSITIVITY-PRESERVATION and high-resolution are two desirable attributes a flux discretization scheme should possess. High-resolution refers to the capability to capture with few nodes continuous and discontinuous waves while not introducing spurious oscillations, and can be achieved through flux or slope limiters. Positivity-preservation refers to the capability to conserve the positivity of the determinative properties. The determinative properties are the properties that must necessarily be positive for the solution to be within physical bounds. For instance, for the Euler equations, the determinative properties are the density and the temperature. For the multi-species Favre-averaged Navier-Stokes equations, not only must the density and the temperature remain positive, but the mass fractions, the turbulence kinetic energy, and the dissipation rate must also remain positive. Should the latter become negative, the solution is not within physically-admissible bounds and severe convergence difficulties can ensue. A method that is positivity-preserving prevents such convergence problems by guaranteeing positivity of the determinative properties.

When solving a scalar advection equation, the Courant upwinded stencil is well-known to conserve the positivity of the variable solved. However, when extended to second-order accuracy, the Courant scheme is not guaranteed to remain positivity-preserving. For instance, in Ref. [1], it is shown that second-order accurate schemes generally do not preserve positivity unless flux limiters are used. As well, in Ref. [2], it is demonstrated that flux limiters are insufficient to guarantee positivity of reacting advection equations, and a new class of flux limited schemes is thus presented that is positivity-preserving in the presence of chemical reactions. The latter methods are, however, limited to scalar conservation laws and do not guarantee positivity-preservation when used to solve a system of conservation laws (i.e. a group of several coupled scalar conservation laws).

When solving systems of conservation laws, most commonly-used flux discretization schemes (Roe, HLL, AUSM, etc) do not generally preserve the positivity of the determinative properties. On the other hand, two schemes that have been shown to be positivity-preserving under a CFL-like condition are the Godunov exact Riemann solver and the Steger-Warming flux vector splitting scheme [3, 4]. The latter are, however, first-order accurate. When extended to second-order accuracy through

*Faculty Member, Dept. of Aerospace Engineering, Pusan National University, Busan 609-735, Korea, http://www.bernardparent.com.

flux limiters or MUSCL slope limiters, the positivity-preserving property is lost. For this reason, much effort has been devoted recently to craft second-order-accurate stencils that are generally positivity-preserving (see for instance Refs. [5, 6, 7, 8]). The latter methods ensure positivity-preservation by reducing the slope limiter function within the MUSCL reconstruction stage. Because the MUSCL slope-limited approach necessarily requires the vector of conserved variables to be reconstructed for every cell interface, it requires more computing work than a flux-limited scheme. Better performance could hence be expected from a flux-limited method over a MUSCL strategy.

In Ref. [9], it is shown that, when used in conjunction with the first-order Steger-Warming scheme, a flux-limited method can preserve positivity under certain conditions. One of these conditions is that the positive and negative flux Jacobian matrices need to be rewritten in symmetric form. The approach follows the work of Friedrichs [10], in which it is proven that the positivity of a system of equations can be preserved when the matrix coefficients multiplying the vector of conserved variables within the discrete equation have positive eigenvalues and are symmetric. This is particularly problematic when trying to craft a positivity-preserving method for compressible flow, because the coefficients yielded by the common discretization methods (such as Steger-Warming, Roe, HLL, etc) are not symmetric. Then, the discretization schemes need to be severely modified to guarantee positivity-preservation. Such modifications can then result in a significant loss of resolution and/or of the desirable monotonic property.

Another approach that has been proposed recently to obtain positivity-preserving flux-limited methods is the so-called "rule of the positive coefficients" [11], which states that positivity is preserved as long as the coefficients of the discrete equation have positive eigenvalues and have the same eigenvectors as those of the corresponding flux Jacobians. The advantage of the rule of the positive coefficients over Friedrichs' scheme is that it can be used in conjunction with some commonly-used discretization methods for compressible flow without requiring a symmetrization of the Jacobian matrices. For instance, using the rule of the positive coefficients, a flux-limited second-order accurate extension of the Steger-Warming scheme was outlined in [11] and denoted as POSFL. The POSFL scheme did not require a modification of the Jacobian matrices and was seen to maintain the monotonicity of the underlying first-order scheme while being second-order accurate and being positivity-preserving. However, POSFL was found to have one substantial drawback compared to the conventional (non-positivity-preserving) TVD schemes: namely, significantly more dissipation is introduced by the stencil in the vicinity of contact discontinuities. This was attributed to the POSFL approach forcing the limiter to be the same over all flux components while the conventional TVD stencils allowed the limiter to have a different value for each flux component (i.e. component-wise flux limiting).

In this paper, a novel positivity-preserving method is proposed for systems of conservation laws that overcomes the shortcomings of previous approaches. The method consists of extending the Steger-Warming scheme to second-order accuracy through the use of a component-wise flux limiter that satisfies the rule of the positive coefficients. The method proposed is monotonicity-preserving, positivity-preserving, and is flux limited (i.e., it does not entail the cumbersome MUSCL reconstruction of the conserved variables at the cell's interfaces). Further, contrarily to the POSFL scheme presented in Ref. [11], the method proposed in this paper does not force the limiter to be the same over all flux components, hence resulting in much improved resolution in the vicinity of contact discontinuities.

2. Class of Systems of Conservation Laws

The schemes presented herein apply to a system of hyperbolic conservation laws of the form:

$$\frac{\partial}{\partial t}U + \frac{\partial}{\partial x}F(U) = 0 \tag{1}$$

where U is the vector of conserved variables and F is the vector of convective fluxes. Further, the system of conservation laws must have the following two properties.

Firstly, the system of conservation laws must be such that the convective flux $F(U)$ is a homogeneous function of degree one in U:

$$F = AU \tag{2}$$

with the convective flux Jacobian $A \equiv \partial F/\partial U$.

Secondly, the system of conservation laws must satisfy the "rule of the positive coefficients". The rule of the positive coefficients can be summarized as follows. Consider an equation in which the vector of conserved variables on node A is determined as a function of the vector of conserved variables on the neighboring nodes B, C, D, etc:

$$C_{\mathrm{A}}U_{\mathrm{A}} = C_{\mathrm{B}}U_{\mathrm{B}} + C_{\mathrm{C}}U_{\mathrm{C}} + C_{\mathrm{D}}U_{\mathrm{D}} + ... \tag{3}$$

where $C_{\mathrm{A,B,C,..}}$ are square matrix coefficients. According to the rule of the positive coefficients, the determinative properties associated with vector U_{A} are guaranteed to be positive if the determinative properties associated with the vectors $U_{\mathrm{B,C,D,...}}$ are positive and if the matrix coefficients $C_{\mathrm{A,B,C,...}}$ are positive. A "determinative property" is defined as a property that must necessarily be positive to yield a vector of conserved variables that is within physically-admissible bounds. For instance, for the Euler equations, the determinative properties would correspond to the temperature and the density. For the multi-species Favre-averaged Navier-Stokes equations, the determinative properties would further include the species partial densities as well as the turbulence kinetic energy and dissipation rate. A coefficient is considered positive if all its eigenvalues are greater than zero and if its eigenvectors are the same as those of the respective convective flux Jacobian:

$$C_{\mathrm{A}} = L^{-1}(U_{\mathrm{A}}) \times D^{+}_{\mathrm{A}} \times L(U_{\mathrm{A}}) \,, \quad C_{\mathrm{B}} = L^{-1}(U_{\mathrm{B}}) \times D^{+}_{\mathrm{B}} \times L(U_{\mathrm{B}}) \,, \quad ... \tag{4}$$

with L the left eigenvector matrix and D^{+} a diagonal matrix with the diagonal elements being greater than zero.

The Euler equations (comprising of the mass conservation, momentum conservation, and total energy conservation equations) have the two properties mentioned above. Indeed, the Euler equations can be shown to have flux vectors that are homogeneous functions of degree one and to satisfy the rule of the positive coefficients [11].

3. Flux Vector Splitting Discretization

When discretizing Eq. (1) on a uniformly spaced mesh using a first-order backward stencil for the time derivative and a conservative stencil for the spatial derivatives, the following is obtained:

$$\frac{U_i^{n+1} - U_i}{\Delta t} + \frac{F_{i+1/2} - F_{i-1/2}}{\Delta x} = 0 \tag{5}$$

For the Steger-Warming flux vector splitting scheme, the flux at the interface becomes [12]:

$$F_{i+1/2} = F_i^{+} + F_{i+1}^{-} \tag{6}$$

where $F^{\pm} \equiv L^{-1}\Lambda^{\pm}LU$ with $\Lambda^{\pm} \equiv \frac{1}{2}(\Lambda \pm |\Lambda|)$. In the latter, Λ is the eigenvalue matrix, L the left eigenvector matrix, and L^{-1} the right eigenvector matrix.

3.1. Entropy Correction

When conservation laws do not include diffusion phenomena, or when the grid is not refined sufficiently to resolve properly the diffusion terms, the discretization of the convection derivatives using the Steger-Warming method can yield a solution that does not satisfy the second law of thermodynamics. This could lead to the formation of entropy-increasing nonphysical phenomena. One way that such nonphysical phenomena can be avoided is by redefining the eigenvalues in the following manner [13]:

$$[\Lambda \pm |\Lambda|]_{r,r} \rightarrow [\Lambda]_{r,r} \pm \sqrt{[\Lambda]_{r,r}^2 + \delta a^2} \tag{7}$$

In the latter, δ is a user-defined positive number typically set to 0.1. It is here preferred to apply the entropy correction to all the eigenvalues even though only the acoustic waves need to be corrected to prevent nonphysical phenomena from forming. Applying the entropy correction to all the eigenvalues does not affect the accuracy of the solution and has the advantage of allowing larger time steps when integrating the equations.

3.2. Second-Order Extension Using a Component-wise Limiter

The flux at the interface can be extended to second-order accuracy using a component-wise limiter as follows:

$$F_{i+1/2} = F_i^{+} + \frac{1}{2}\Phi^{+}_{i+1/2}\left(F_i^{+} - F_{i-1}^{+}\right) + F_{i+1}^{-} + \frac{1}{2}\Phi^{-}_{i+1/2}\left(F_{i+1}^{-} - F_{i+2}^{-}\right) \tag{8}$$

In the latter, the flux limiter matrix Φ is a diagonal matrix with the elements on the diagonal being greater or equal to 0 and less or equal to 2. By setting the limiter matrix to the identity matrix (i.e. $\Phi^{\pm} = I$), a piecewise-linear distribution of the convective fluxes is in effect, hence resulting in a second-order-accurate scheme. On the other hand, setting the flux limiter matrix to zero (i.e. $\Phi^{\pm} = 0$) yields a first-order-accurate scheme by forcing a piecewise-constant spatial distribution of the convective fluxes.

Because the diagonal elements of the limiter matrix are not necessarily equal to each other, it is possible to limit each flux component independently (i.e. component-wise flux limiting).

For a scalar conservation law, the monotonicity of the solution can be preserved by imposing the Total Variation Diminishing (TVD) condition on the limiter. For a system of conservation laws, it is a common practice to impose the TVD condition on each flux component, independently of the other components (while this does not guarantee monotonicity-preservation of all properties per se, this yields a solution that is close to being monotonicity-preserving). This can be done by setting the diagonal elements of the limiter matrices Φ^+ and Φ^- as follows:

$$\left[\Phi^-_{i+1/2}\right]_{r,r} = \phi\left(\frac{\left[F^-_i\right]_r - \left[F^-_{i+1}\right]_r}{\left[F^-_{i+1}\right]_r - \left[F^-_{i+2}\right]_r}\right) \tag{9}$$

$$\left[\Phi^+_{i+1/2}\right]_{r,r} = \phi\left(\frac{\left[F^+_{i+1}\right]_r - \left[F^+_i\right]_r}{\left[F^+_i\right]_r - \left[F^+_{i-1}\right]_r}\right) \tag{10}$$

where ϕ is the limiter function. The limiter function must fall within a certain admissible limiter region to yield high-resolution TVD schemes. Three such limiter functions are the Van Leer, minmod, and superbee limiters [14, 15]:

$$\phi(b) = \begin{cases} \max\left(0,\ \min\left(1,\ b\right)\right) & \text{(minmod)} \\ \left(b + |b|\right)/\left(1 + |b|\right) & \text{(Van Leer)} \\ \max\left(0,\ \min\left(2,\ b\right),\ \min\left(1,\ 2b\right)\right) & \text{(superbee)} \end{cases} \tag{11}$$

When used in conjunction with Eq. (8) the latter limiter functions have the property to yield symmetric discretization stencils. That is, the discretization stencils are such that the discrete solution of a leftward-travelling wave is symmetric to the one of a rightward-travelling wave.

For reasons that will become clear in subsequent sections, the flux at the interface can also be written as follows:

$$F_{i+1/2} = F^+_i + \frac{1}{2}L_i^{-1}\Psi^+_{i+1/2}\left(G^+_i - G^+_{i-1}\right) + F^-_{i+1} + \frac{1}{2}L_{i+1}^{-1}\Psi^-_{i+1/2}\left(G^-_{i+1} - G^-_{i+2}\right) \tag{12}$$

where Ψ^+ and Ψ^- are diagonal matrices and where G is the product between the eigenvalues and the characteristic variables:

$$G^\pm \equiv \Lambda^\pm L U \tag{13}$$

Because Eq. (12) must yield the same flux at the interface as Eq. (8), we can equate both equations to obtain:

$$\frac{1}{2}\Phi^+_{i+1/2}\left(F^+_i - F^+_{i-1}\right) + \frac{1}{2}\Phi^-_{i+1/2}\left(F^-_{i+1} - F^-_{i+2}\right) = \frac{1}{2}L_i^{-1}\Psi^+_{i+1/2}\left(G^+_i - G^+_{i-1}\right) + \frac{1}{2}L_{i+1}^{-1}\Psi^-_{i+1/2}\left(G^-_{i+1} - G^-_{i+2}\right) \tag{14}$$

Then, noting that $\Phi^+_{i+1/2}$ and $\Phi^-_{i+1/2}$ are independent of each other and that $\Psi^+_{i+1/2}$ and $\Psi^-_{i+1/2}$ are also independent of each other, it follows that the following two equations must hold:

$$L_i^{-1}\Psi^+_{i+1/2}\left(G^+_i - G^+_{i-1}\right) = \Phi^+_{i+1/2}\left(F^+_i - F^+_{i-1}\right) \tag{15}$$

$$L_{i+1}^{-1}\Psi^-_{i+1/2}\left(G^-_{i+1} - G^-_{i+2}\right) = \Phi^-_{i+1/2}\left(F^-_{i+1} - F^-_{i+2}\right) \tag{16}$$

The former can yield an expression for Ψ^+ by multiplying both sides by L_i, writing in tensor form, and then isolating the diagonal elements of the Ψ matrix:

$$\left[\Psi^+_{i+1/2}\right]_{r,r} = \frac{\left[L_i\Phi^+_{i+1/2}\left(F^+_i - F^+_{i-1}\right)\right]_r}{\left[G^+_i - G^+_{i-1}\right]_r} \tag{17}$$

Similarly, we can find an expression for the Ψ^- diagonal elements:

$$\left[\Psi^-_{i+1/2}\right]_{r,r} = \frac{\left[L_{i+1}\Phi^-_{i+1/2}\left(F^-_{i+1} - F^-_{i+2}\right)\right]_r}{\left[G^-_{i+1} - G^-_{i+2}\right]_r} \tag{18}$$

It is emphasized that as long as $\Psi^\pm$ is defined according to Eqs. (17)-(18), the flux at the interface determined from Eq. (12) is equivalent to the flux at the interface determined from Eq. (8). Writing the flux at the interface as in Eq. (12) has some advantages, as will become apparent when crafting positivity-preserving discretization stencils in Section 5 below.

4. Necessary Conditions for Positivity-preservation

The rule of the positive coefficients is now used to determine the restrictions on the limiter matrices and on the time step which ensure positivity-preservation. It is noted that the conditions derived in this section apply to a *component-wise* flux limiter function. That is, the limiter function is not necessarily constant over all flux components. Because of this, the positivity-preserving restrictions on the maximum allowable time step and on the limiter function found herein differ significantly than those outlined in Ref. [11], in which the limiter function was assumed constant over all flux components.

The positivity-preserving conditions applicable to a component-wise flux limiter can be found from the rule of the positive coefficients as follows. First, we obtain a second-order accurate discrete equation by substituting the second-order accurate flux at the interface outlined in Eq. (12) into the discrete equation (5):

$$\begin{aligned}\frac{\Delta x}{\Delta t}\left(U_i^{n+1}-U_i\right) = &-F_i^+ - \frac{1}{2}L_i^{-1}\Psi_{i+1/2}^+\left(G_i^+ - G_{i-1}^+\right) - F_{i+1}^- - \frac{1}{2}L_{i+1}^{-1}\Psi_{i+1/2}^-\left(G_{i+1}^- - G_{i+2}^-\right)\\ &+ F_{i-1}^+ + \frac{1}{2}L_{i-1}^{-1}\Psi_{i-1/2}^+\left(G_{i-1}^+ - G_{i-2}^+\right) + F_i^- + \frac{1}{2}L_i^{-1}\Psi_{i-1/2}^-\left(G_i^- - G_{i+1}^-\right)\end{aligned} \tag{19}$$

Noting that $F^\pm = L^{-1}\Lambda^\pm LU$ and that $G^\pm = \Lambda^\pm LU$, the latter can also be written as:

$$C_i^{n+1}U_i^{n+1} = C_{i-2}U_{i-2} + C_{i-1}U_{i-1} + C_iU_i + C_{i+1}U_{i+1} + C_{i+2}U_{i+2} \tag{20}$$

in which the matrices C_i, C_{i-1}, etc correspond to the discretization coefficients and are defined as:

$$C_i^{n+1} \equiv \frac{\Delta x}{\Delta t}I = \frac{\Delta x}{\Delta t}(L_i^{-1})^{n+1}IL_i^{n+1} \tag{21}$$

$$C_i \equiv L_i^{-1}\left(\frac{\Delta x}{\Delta t}I - \Lambda_i^+ - \frac{1}{2}\Psi_{i+1/2}^+\Lambda_i^+ + \Lambda_i^- + \frac{1}{2}\Psi_{i-1/2}^-\Lambda_i^-\right)L_i \tag{22}$$

$$C_{i-1} \equiv \left(L_{i-1}^{-1} + \frac{1}{2}L_i^{-1}\Psi_{i+1/2}^+ + \frac{1}{2}L_{i-1}^{-1}\Psi_{i-1/2}^+\right)\Lambda_{i-1}^+L_{i-1} \tag{23}$$

$$C_{i+1} \equiv -\left(L_{i+1}^{-1} + \frac{1}{2}L_{i+1}^{-1}\Psi_{i+1/2}^- + \frac{1}{2}L_i^{-1}\Psi_{i-1/2}^-\right)\Lambda_{i+1}^-L_{i+1} \tag{24}$$

$$C_{i-2} \equiv -\frac{1}{2}L_{i-1}^{-1}\Psi_{i-1/2}^+\Lambda_{i-2}^+L_{i-2} \tag{25}$$

$$C_{i+2} \equiv \frac{1}{2}L_{i+1}^{-1}\Psi_{i+1/2}^-\Lambda_{i+2}^-L_{i+2} \tag{26}$$

To obtain a positivity-preserving discretization stencil, the rule of the positive coefficients must be satisfied. The first constraint imposed by the rule of the positive coefficients is that the eigenvectors of the coefficients must match those of the corresponding flux Jacobian. Such is not the case for all coefficients. In fact, only the coefficients C_i and C_i^{n+1} satisfy this condition.

It follows that the discrete equation (20) can not satisfy the rule of the positive coefficients directly. Rather, to satisfy the rule of the positive coefficients, it is necessary to first rewrite the discrete equation (20) as:

$$C_i^{n+1}U_i^{n+1} = C_i'U_i + C_{i+1}'U_{i+1} + C_{i-1}'U_{i-1} \tag{27}$$

In the latter, the coefficient C_i^{n+1} is as defined above while the coefficients C_i', C_{i-1}' and C_{i+1}' are such that the following equations hold:

$$C_i'U_i \equiv L_i^{-1}\left(\frac{\Delta x}{\Delta t}I - \Lambda_i^+ - \frac{1}{2}\Psi_{i+1/2}^+\Lambda_i^+ + \Lambda_i^- + \frac{1}{2}\Psi_{i-1/2}^-\Lambda_i^-\right)L_iU_i + \frac{1}{2}L_i^{-1}\Psi_{i+1/2}^+G_{i-1}^+ - \frac{1}{2}L_i^{-1}\Psi_{i-1/2}^-G_{i+1}^- \tag{28}$$

$$C_{i-1}'U_{i-1} \equiv \left(L_{i-1}^{-1} + \frac{1}{2}L_{i-1}^{-1}\Psi_{i-1/2}^+\right)G_{i-1}^+ - \frac{1}{2}L_{i-1}^{-1}\Psi_{i-1/2}^+G_{i-2}^+ \tag{29}$$

$$C_{i+1}'U_{i+1} \equiv -\left(L_{i+1}^{-1} + \frac{1}{2}L_{i+1}^{-1}\Psi_{i+1/2}^-\right)G_{i+1}^- + \frac{1}{2}L_{i+1}^{-1}\Psi_{i+1/2}^-G_{i+2}^- \tag{30}$$

In Eq. (27) the coefficient C_i^{n+1} satisfies the rule of the positive coefficients by having eigenvectors equal to the ones of the corresponding convective flux Jacobian and by having positive eigenvalues. On the other hand, the other three coefficients (C_i', C_{i-1}' and C_{i+1}') are not generally positive but can become positive under certain conditions.

4.1. Positivity-preserving Restrictions on the Flux Limiter

Let's now proceed to find the conditions for which the coefficients C'_{i-1} and C'_{i+1} are positive. Such will yield restrictions on the diagonal matrices Ψ^+ and Ψ^-, which themselves will lead to restrictions on the flux limiter through Eqs. (17) and (18). The positivity-preserving restriction on the Ψ^- matrix can be determined from Eq. (30) by rewriting the coefficient C'_{i+1} in terms of eigenvectors and eigenvalues:

$$L^{-1}_{i+1} D^+_{i+1} L_{i+1} U_{i+1} = -L^{-1}_{i+1} \left(I + \frac{1}{2} \Psi^-_{i+1/2} \right) G^-_{i+1} + \frac{1}{2} L^{-1}_{i+1} \Psi^-_{i+1/2} G^-_{i+2} \tag{31}$$

Multiply all terms by $2L_{i+1}$ and write in tensor form:

$$2 \left[D^+_{i+1} \right]_{r,r} \left[L_{i+1} U_{i+1} \right]_r = - \left[2I + \Psi^-_{i+1/2} \right]_{r,r} \left[G^-_{i+1} \right]_r + \left[\Psi^-_{i+1/2} \right]_{r,r} \left[G^-_{i+2} \right]_r \tag{32}$$

Multiply all terms by $\left[\Lambda^-_{i+1} \right]_{r,r}$:

$$2 \left[D^+_{i+1} \right]_{r,r} \left[G^-_{i+1} \right]_r = - \left[2I + \Psi^-_{i+1/2} \right]_{r,r} \left[\Lambda^-_{i+1} \right]_{r,r} \left[G^-_{i+1} \right]_r + \left[\Psi^-_{i+1/2} \right]_{r,r} \left[\Lambda^-_{i+1} \right]_{r,r} \left[G^-_{i+2} \right]_r \tag{33}$$

Divide all terms by $\left[G^-_{i+1} \right]_r$:

$$2 \left[D^+_{i+1} \right]_{r,r} = - \left[2I + \Psi^-_{i+1/2} \right]_{r,r} \left[\Lambda^-_{i+1} \right]_{r,r} + \left[\Psi^-_{i+1/2} \right]_{r,r} \left[\Lambda^-_{i+1} \right]_{r,r} \frac{\left[G^-_{i+2} \right]_r}{\left[G^-_{i+1} \right]_r} \tag{34}$$

For the stencil to be positivity-preserving, all the diagonal elements within the matrix D^+_{i+1} must be positive. Therefore, it follows that:

$$- \left[2I + \Psi^-_{i+1/2} \right]_{r,r} \left[\Lambda^-_{i+1} \right]_{r,r} + \left[\Psi^-_{i+1/2} \right]_{r,r} \left[\Lambda^-_{i+1} \right]_{r,r} \frac{\left[G^-_{i+2} \right]_r}{\left[G^-_{i+1} \right]_r} > 0 \tag{35}$$

Divide all terms by $\left[\Lambda^-_{i+1} \right]_{r,r}$ noting that $\left[\Lambda^-_{i+1} \right]_{r,r}$ is always negative ($[\Lambda^-]_{r,r}$ can not be zero because of the entropy correction Eq. (7)):

$$- \left[2I + \Psi^-_{i+1/2} \right]_{r,r} + \left[\Psi^-_{i+1/2} \right]_{r,r} \frac{\left[G^-_{i+2} \right]_r}{\left[G^-_{i+1} \right]_r} < 0 \tag{36}$$

Regroup similar terms:

$$\left[\Psi^-_{i+1/2} \right]_{r,r} \frac{\left[G^-_{i+2} \right]_r - \left[G^-_{i+1} \right]_r}{\left[G^-_{i+1} \right]_r} < 2 \tag{37}$$

If the LHS is negative, the condition is always satisfied. It follows that the condition remains valid if the LHS is subject to the absolute value operator:

$$\left| \left[\Psi^-_{i+1/2} \right]_{r,r} \frac{\left[G^-_{i+2} \right]_r - \left[G^-_{i+1} \right]_r}{\left[G^-_{i+1} \right]_r} \right| < 2 \tag{38}$$

By applying the absolute value operator on the LHS, the range of admissible Ψ^- is further limited, and this results in a more dissipative stencil. However, as shall be seen in the next section (in which the positivity-preserving condition on the time step is derived), it is necessary to do so to ensure that the stencil remains positivity-preserving for a small time step.

Condition (38) can also be rewritten as follows:

$$- \left| \frac{2 \left[G^-_{i+1} \right]_r}{\left[G^-_{i+2} \right]_r - \left[G^-_{i+1} \right]_r} \right| < \left[\Psi^-_{i+1/2} \right]_{r,r} < \left| \frac{2 \left[G^-_{i+1} \right]_r}{\left[G^-_{i+2} \right]_r - \left[G^-_{i+1} \right]_r} \right| \tag{39}$$

Starting from Eq. (29) and following similar steps, we can find the condition on the diagonal matrix Ψ^+ that ensures that the coefficient C'_{i-1} is positive. This yields:

$$\left| \left[\Psi^+_{i-1/2} \right]_{r,r} \frac{\left[G^+_{i-2} \right]_r - \left[G^+_{i-1} \right]_r}{\left[G^+_{i-1} \right]_r} \right| < 2 \tag{40}$$

which can be rewritten to:

$$- \left| \frac{2 \left[G^+_{i-1} \right]_r}{\left[G^+_{i-2} \right]_r - \left[G^+_{i-1} \right]_r} \right| < \left[\Psi^+_{i-1/2} \right]_{r,r} < \left| \frac{2 \left[G^+_{i-1} \right]_r}{\left[G^+_{i-2} \right]_r - \left[G^+_{i-1} \right]_r} \right| \tag{41}$$

For a conservative stencil, the Ψ matrix at the $i+1/2$ interface must be determined in the same way as the Ψ matrix at the $i-1/2$ interface:

$$-\left|\frac{2\left[G_i^+\right]_r}{\left[G_{i-1}^+\right]_r-\left[G_i^+\right]_r}\right| < \left[\Psi_{i+1/2}^+\right]_{r,r} < \left|\frac{2\left[G_i^+\right]_r}{\left[G_{i-1}^+\right]_r-\left[G_i^+\right]_r}\right| \tag{42}$$

In summary, it can be stated that, should the flux at the interface be determined as in Eq. (12), conditions (39) and (42) must be satisfied in order to guarantee a positivity-preserving stencil.

4.2. Positivity-preserving Restriction on the Time Step

The rule of the positive coefficients can also be used to determine the maximum time step that guarantees positivity-preservation. This can be done by starting from Eq. (28), rewriting the coefficient in terms of eigenvectors, multiplying all terms by L_i, and then rewriting in tensor form:

$$\begin{aligned}\left[D_i^+\right]_{r,r}\left[L_iU_i\right]_r = &\left[\frac{\Delta x}{\Delta t}I-\Lambda_i^+-\frac{1}{2}\Psi_{i+1/2}^+\Lambda_i^++\Lambda_i^-+\frac{1}{2}\Psi_{i-1/2}^-\Lambda_i^-\right]_{r,r}\left[L_iU_i\right]_r+\frac{1}{2}\left[\Psi_{i+1/2}^+\right]_{r,r}\left[G_{i-1}^+\right]_r\\ &-\frac{1}{2}\left[\Psi_{i-1/2}^-\right]_{r,r}\left[G_{i+1}^-\right]_r\end{aligned} \tag{43}$$

Regroup similar terms together:

$$\left[D_i^+\right]_{r,r}\left[L_iU_i\right]_r=\left[\frac{\Delta x}{\Delta t}I-\Lambda_i^++\Lambda_i^-\right]_{r,r}\left[L_iU_i\right]_r+\frac{1}{2}\left[\Psi_{i+1/2}^+\right]_{r,r}\left[G_{i-1}^+-G_i^+\right]_r+\frac{1}{2}\left[\Psi_{i-1/2}^-\right]_{r,r}\left[G_i^--G_{i+1}^-\right]_r \tag{44}$$

Multiply all terms by $[\Lambda_i^+]_{r,r}$:

$$\begin{aligned}\left[D_i^+\right]_{r,r}\left[G_i^+\right]_r=&\left[\frac{\Delta x}{\Delta t}I-\Lambda_i^++\Lambda_i^-\right]_{r,r}\left[G_i^+\right]_r+\frac{1}{2}\left[\Psi_{i+1/2}^+\right]_{r,r}\left[G_{i-1}^+-G_i^+\right]_r\left[\Lambda_i^+\right]_{r,r}\\ &+\frac{1}{2}\left[\Psi_{i-1/2}^-\right]_{r,r}\left[G_i^--G_{i+1}^-\right]_r\left[\Lambda_i^+\right]_{r,r}\end{aligned} \tag{45}$$

Divide all terms by $[G_i^+]_r$:

$$\left[D_i^+\right]_{r,r}=\left[\frac{\Delta x}{\Delta t}I-\Lambda_i^++\Lambda_i^-\right]_{r,r}+\frac{1}{2}\left[\Psi_{i+1/2}^+\right]_{r,r}\frac{\left[G_{i-1}^+-G_i^+\right]_r}{\left[G_i^+\right]_r}\left[\Lambda_i^+\right]_{r,r}+\frac{1}{2}\left[\Psi_{i-1/2}^-\right]_{r,r}\frac{\left[G_i^--G_{i+1}^-\right]_r}{\left[G_i^+\right]_r}\left[\Lambda_i^+\right]_{r,r} \tag{46}$$

Now note that $[G_i^+]_r=[\Lambda_i^+]_{r,r}[L_iU_i]_r=[\Lambda_i^+]_{r,r}[G_i^-]_r/[\Lambda_i^-]_{r,r}$:

$$\left[D_i^+\right]_{r,r}=\left[\frac{\Delta x}{\Delta t}I-\Lambda_i^++\Lambda_i^-\right]_{r,r}+\frac{1}{2}\left[\Psi_{i+1/2}^+\right]_{r,r}\frac{\left[G_{i-1}^+-G_i^+\right]_r}{\left[G_i^+\right]_r}\left[\Lambda_i^+\right]_{r,r}-\frac{1}{2}\left[\Psi_{i-1/2}^-\right]_{r,r}\frac{\left[G_{i+1}^--G_i^-\right]_r}{[G_i^-]_r}\left[\Lambda_i^-\right]_{r,r} \tag{47}$$

To satisfy the rule of the positive coefficients, all the terms on the diagonal of the matrix D_i^+ must be positive. Then, it follows that:

$$\left[\frac{\Delta x}{\Delta t}I-\Lambda_i^++\Lambda_i^-\right]_{r,r}+\frac{1}{2}\left[\Psi_{i+1/2}^+\right]_{r,r}\frac{\left[G_{i-1}^+-G_i^+\right]_r}{\left[G_i^+\right]_r}\left[\Lambda_i^+\right]_{r,r}-\frac{1}{2}\left[\Psi_{i-1/2}^-\right]_{r,r}\frac{\left[G_{i+1}^--G_i^-\right]_r}{[G_i^-]_r}\left[\Lambda_i^-\right]_{r,r}>0 \tag{48}$$

Without loss of generality, it can also be stated that:

$$\left[\frac{\Delta x}{\Delta t}I-\Lambda_i^++\Lambda_i^-\right]_{r,r}-\frac{1}{2}\left|\left[\Psi_{i+1/2}^+\right]_{r,r}\frac{\left[G_{i-1}^+-G_i^+\right]_r}{\left[G_i^+\right]_r}\right|\left[\Lambda_i^+\right]_{r,r}+\frac{1}{2}\left|\left[\Psi_{i-1/2}^-\right]_{r,r}\frac{\left[G_{i+1}^--G_i^-\right]_r}{[G_i^-]_r}\right|\left[\Lambda_i^-\right]_{r,r}>0 \tag{49}$$

The most restrictive condition would occur when the absolute value terms are as high as possible. But, according to the positivity conditions (38) and (40), the magnitude of these terms can be at most 2. Then:

$$\left[\frac{\Delta x}{\Delta t}I-\Lambda_i^++\Lambda_i^-\right]_{r,r}-\left[\Lambda_i^+\right]_{r,r}+\left[\Lambda_i^-\right]_{r,r}>0 \tag{50}$$

or, noting that $\Lambda^{\pm} = \frac{1}{2}(\Lambda \pm |\Lambda|)$ and isolating the time step, we get:

$$\Delta t < \frac{\Delta x}{2\left|[\Lambda_i]_{r,r}\right|} \quad \forall r, \forall i \tag{51}$$

Thus, we find a condition on the time step that must be enforced to guarantee positivity-preservation. That is, the time step must be less than half the ratio between the grid spacing and the largest eigenvalue (in magnitude) within the domain. For the Euler equations, this can be easily shown to yield a restriction on the Courant number. That is, the maximum Courant number within the domain should be less than 1/2 to guarantee positivity-preservation.

In summary, the discretization stencil is guaranteed to be positivity-preserving if conditions (39), (42), and (51) are satisfied conjunctly. Should either one of these conditions not be satisfied, there is no guarantee that the stencil will conserve the positivity of the determinative properties.

5. Proposed Positivity-preserving High-resolution Schemes

A novel class of flux-limited schemes is now outlined that is high-resolution while satisfying the positivity-preserving conditions outlined in the previous section. The difficulty in achieving this task lies in determining the optimal limiter that is low enough to yield a positivity-preserving scheme while being sufficiently high to yield a high-resolution scheme. For this purpose, it is convenient to express the flux at the interface as in Eq. (12):

$$F_{i+1/2} = F_i^+ + \frac{1}{2}L_i^{-1}\Psi_{i+1/2}^+\left(G_i^+ - G_{i-1}^+\right) + F_{i+1}^- + \frac{1}{2}L_{i+1}^{-1}\Psi_{i+1/2}^-\left(G_{i+1}^- - G_{i+2}^-\right) \tag{52}$$

where $G^{\pm} = \Lambda^{\pm}LU$, $F^{\pm} = L^{-1}G^{\pm}$, $\Lambda^{\pm} = \frac{1}{2}(\Lambda \pm |\Lambda|)$, L the left eigenvector matrix, L^{-1} the right eigenvector matrix, Λ the eigenvalue matrix, U the vector of conserved variables, and $\Psi^{\pm}$ some diagonal matrices. In order to obtain a positivity-preserving scheme that is as close as possible to the standard flux limited Steger-Warming method [see Eq. (8)], the diagonal matrix Ψ^- should be as close as possible to the one obtained in Eq. (18) while being within the bounds imposed by the positivity-preserving condition (39). This can be accomplished as follows:

$$\left[\Psi_{i+1/2}^-\right]_{r,r} = \max\left(-\left|\frac{\xi\left[G_{i+1}^-\right]_r}{\left[G_{i+1}^- - G_{i+2}^-\right]_r}\right|, \min\left(\frac{\left[L_{i+1}\Phi_{i+1/2}^-\left(F_{i+1}^- - F_{i+2}^-\right)\right]_r}{\left[G_{i+1}^- - G_{i+2}^-\right]_r}, \left|\frac{\xi\left[G_{i+1}^-\right]_r}{\left[G_{i+1}^- - G_{i+2}^-\right]_r}\right|\right)\right) \tag{53}$$

And similarly, the matrix Ψ^+ that is as close as possible to the expression (17) while being within the bounds imposed by the positivity-preserving condition (42) corresponds to:

$$\left[\Psi_{i+1/2}^+\right]_{r,r} = \max\left(-\left|\frac{\xi\left[G_i^+\right]_r}{\left[G_i^+ - G_{i-1}^+\right]_r}\right|, \min\left(\frac{\left[L_i\Phi_{i+1/2}^+\left(F_i^+ - F_{i-1}^+\right)\right]_r}{\left[G_i^+ - G_{i-1}^+\right]_r}, \left|\frac{\xi\left[G_i^+\right]_r}{\left[G_i^+ - G_{i-1}^+\right]_r}\right|\right)\right) \tag{54}$$

where the limiter matrices Φ^- and Φ^+ are determined as in Eqs. (9) and (10):

$$\left[\Phi_{i+1/2}^-\right]_{r,r} = \phi\left(\frac{\left[F_i^-\right]_r - \left[F_{i+1}^-\right]_r}{\left[F_{i+1}^-\right]_r - \left[F_{i+2}^-\right]_r}\right) \quad \text{and} \quad \left[\Phi_{i+1/2}^+\right]_{r,r} = \phi\left(\frac{\left[F_{i+1}^+\right]_r - \left[F_i^+\right]_r}{\left[F_i^+\right]_r - \left[F_{i-1}^+\right]_r}\right) \tag{55}$$

where ϕ is the flux limiter function (minmod, Van Leer, superbee, etc) as specified in Eq. (11):

$$\phi(b) = \begin{cases} \max(0,\ \min(1,\ b)) & \text{(minmod)} \\ (b + |b|)/(1 + |b|) & \text{(Van Leer)} \\ \max(0,\ \min(2,\ b),\ \min(1,\ 2b)) & \text{(superbee)} \end{cases} \tag{56}$$

The schemes outlined above achieve high resolution through the use of component-wise flux limiting and are guaranteed to be positivity-preserving as long as the user-specified constant ξ is within the following range:

$$0 < \xi < 2 \tag{57}$$

The higher ξ is, the less dissipative the stencil becomes. Because of round-off errors due to the use of real or double precision numbers, and because of small errors due to compiler optimization, ξ should be set to a value slightly below 2. For the 1D problems considered herein, ξ can be set to as high 1.99 without resulting in negative internal energies or densities. However, for certain 2D or 3D problems, it is necessary to decrease ξ further. As well, it is found that fixing ξ to a value 10% less than its theoretical maximum helps to prevent divergence at high time steps. For these reasons, ξ is set to 1.8 for all test cases here considered.

6. Test Cases

Several test cases with particularly stringent conditions are now considered to assess the capability of the proposed schemes to maintain positivity of the determinative properties. As well, a comparison with the standard TVD stencils is presented to assess the amount of resolution lost through the enforcement of positivity-preservation. Firstly, some test cases are presented solving the one-dimensional Euler equations in Cartesian coordinates. This is followed by test cases focused on the solution of the 2D and 3D Euler equations in generalized curvilinear coordinates.

6.1. One-Dimensional Euler Flow

The performance of the proposed schemes is first assessed in solving the 1D time-accurate Euler equations:

$$\frac{\partial U}{\partial t} + \frac{\partial F}{\partial x} = 0 \tag{58}$$

where the vector of conserved variables U, convective flux vector F and the eigenvectors and eigenvalues of the convective flux Jacobian can be found in the appendix. The solution is advanced accurately in time through a first-order-accurate explicit Euler strategy:

$$\frac{1}{\Delta t}\left(U_i^{n+1} - U_i^n\right) + \frac{1}{\Delta x}\left(F_{i+1/2} - F_{i-1/2}\right) = 0 \tag{59}$$

where the convective flux at the interface, $F_{i+1/2}$, is obtained following the method outlined in Section 5 [see Eqs. (52)-(57)].

Several time-accurate 1D test cases are considered, with the initial conditions outlined in Table 1. For all cases, the specific heat ratio is fixed to 1.4 and the gas constant is set to 286 J/kgK. As revealed in Table 2, negative pressures and densities appear in the solution obtained using well-established flux discretization methods. For instance, both the first-order-accurate Roe scheme [16] and the second-order accurate Yee-Roe scheme [17] (the latter corresponds to a second-order extension of the Roe scheme through a minmod limiter applied to the characteristic variables) fail to maintain positivity when either vacuum is created within the gas or when rarefaction fans of moderate strength make the density decrease significantly. This problem can not be fixed by lowering the time step: even when the time step is such that the maximum Courant number everywhere in the domain is less than 0.001, the Roe schemes do not maintain positivity.

The lack of positivity-preservation is also exhibited by some second-order extensions of the Steger-Warming flux vector splitting method. As outlined in Table 2, a second-order extension of the Steger-Warming scheme through flux limiters is seen to yield negative internal energies when either strong rarefaction waves decrease the density to low values or when a Riemann problem occurs on a flow moving at hypervelocities. In those situations, the flux-limited Steger-Warming scheme is not positivity-preserving, independently of the time step or limiter used. In fact, even the most diffusive TVD limiter is seen not to preserve the positivity of the determinative properties.

Alternately, a second-order accurate extension of the Steger-Warming method can be obtained using the MUSCL strategy [18]. The MUSCL approach achieves second-order accuracy by applying the TVD limiters on the primitive variables instead of the fluxes, and then reconstructing the flux vectors at the cell's interfaces from those extrapolated primitive variables. In so-doing, the flux discretization scheme becomes positivity-preserving, at least when the minmod limiter is used. However, when using more compressive limiters, numerical tests show that MUSCL is not generally positivity-preserving (see Table 2).

TABLE 1.
List of 1D test cases and initial conditions.[a]

		Left initial state ($x \leq 0$)			Right initial state ($x > 0$)		
Case	Description	ρ, kg/m^3	u, m/s	P, bar	ρ, kg/m^3	u, m/s	P, bar
#1	Riemann problem	1	0	1	1	0	0.1
#2	Riemann problem at hypervelocities	1	1600	10	1	1600	0.1
#3	Vacuum generation	1	-1000	0.1	1	1000	0.1
#4	Vacuum generation at hypervelocities	1	1000	0.1	1	3000	0.1
#5	Shock reflection	1	1000	0.1	1	-1000	0.1
#6	Shock reflection at hypervelocities	1	3000	0.1	1	1000	0.1
#7	Double rarefaction waves	1	-200	0.1	1	200	0.1

[a] In all cases, the computational domain is located within $-0.5\,\text{m} \leq x \leq 0.5\,\text{m}$.

TABLE 2.
Assessment of positivity-preserving capability of various schemes when solving the 1D test cases.[a]

	Positivity Preserving?													
	CFL=0.001[b,c]							CFL=0.5[d]						
Method	Case #1	#2	#3	#4	#5	#6	#7	Case #1	#2	#3	#4	#5	#6	#7
Roe (first-order)	Yes	Yes	No	Yes	Yes	Yes	No	Yes	Yes	No	Yes	Yes	Yes	No
Steger-Warming (first-order)	Yes	Yes	Yes	Yes	Yes	Yes	Yes	Yes	Yes	Yes	Yes	Yes	Yes	Yes
Yee-Roe (minmod)	Yes	Yes	No	Yes	Yes	Yes	No	Yes	Yes	No	No	Yes	No	No
S-W flux limited (minmod)	Yes	No	No	Yes	Yes	No	Yes	Yes	No	No	No	Yes	No	Yes
S-W flux limited (Van Leer)	Yes	No	No	No	Yes	No	Yes	Yes	No	No	No	Yes	No	Yes
S-W flux limited (superbee)	Yes	No	No	No	Yes	No	Yes	Yes	No	No	No	No	No	Yes
S-W MUSCL (minmod)	Yes	Yes	Yes	Yes	Yes	Yes	Yes	Yes	Yes	Yes	No	Yes	Yes	Yes
S-W MUSCL (Van Leer)	Yes	Yes	No	Yes	Yes	Yes	Yes	Yes	Yes	No	No	Yes	No	Yes
S-W MUSCL (superbee)	Yes	Yes	No	No	Yes	Yes	Yes	Yes	Yes	No	No	Yes	No	Yes
proposed method (minmod)	Yes	Yes	Yes	Yes	Yes	Yes	Yes	Yes	Yes	Yes	Yes	Yes	Yes	Yes
proposed method (Van Leer)	Yes	Yes	Yes	Yes	Yes	Yes	Yes	Yes	Yes	Yes	Yes	Yes	Yes	Yes
proposed method (superbee)	Yes	Yes	Yes	Yes	Yes	Yes	Yes	Yes	Yes	Yes	Yes	Yes	Yes	Yes

[a] For all cases, the grid is made of 500 equally-spaced nodes.
[b] The time step is constant for all nodes and is such that the maximum Courant number is 0.001 within the domain.
[c] Setting the CFL to a value of 0.1 yields the same outcome.
[d] The time step is constant for all nodes and is such that the maximum Courant number is 0.5 within the domain.

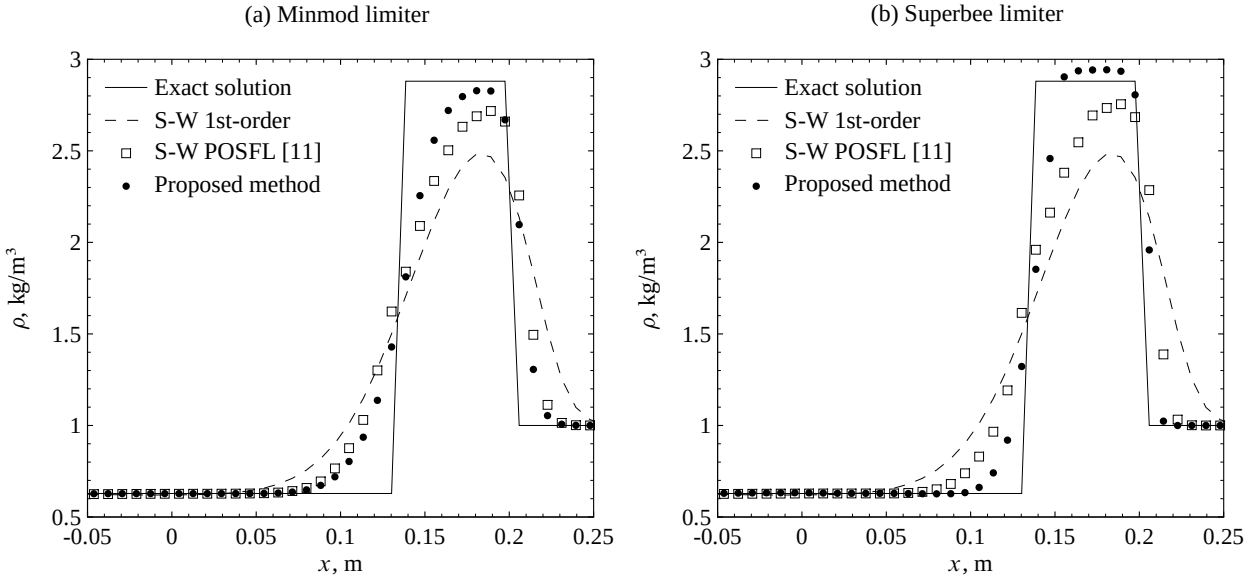

FIGURE 1. Comparison between the proposed schemes and the POSFL schemes [11] on the basis of density profiles for test case #1. The density profiles are obtained using a 120-node grid at a time of 0.8 ms using a time step size such that the maximum Courant number within the domain is 0.1.

As predicted theoretically in the previous sections, the method presented herein does preserve the positivity of the determinative properties as long as the Courant number is less than 0.5. This is verified to be the case even for the most compressive TVD limiter (superbee). Additional test cases reveal that the condition on the Courant number is not aleatory. Indeed, should the time step be such that the Courant number slightly exceeds 0.5 somewhere in the domain, negative internal energies or

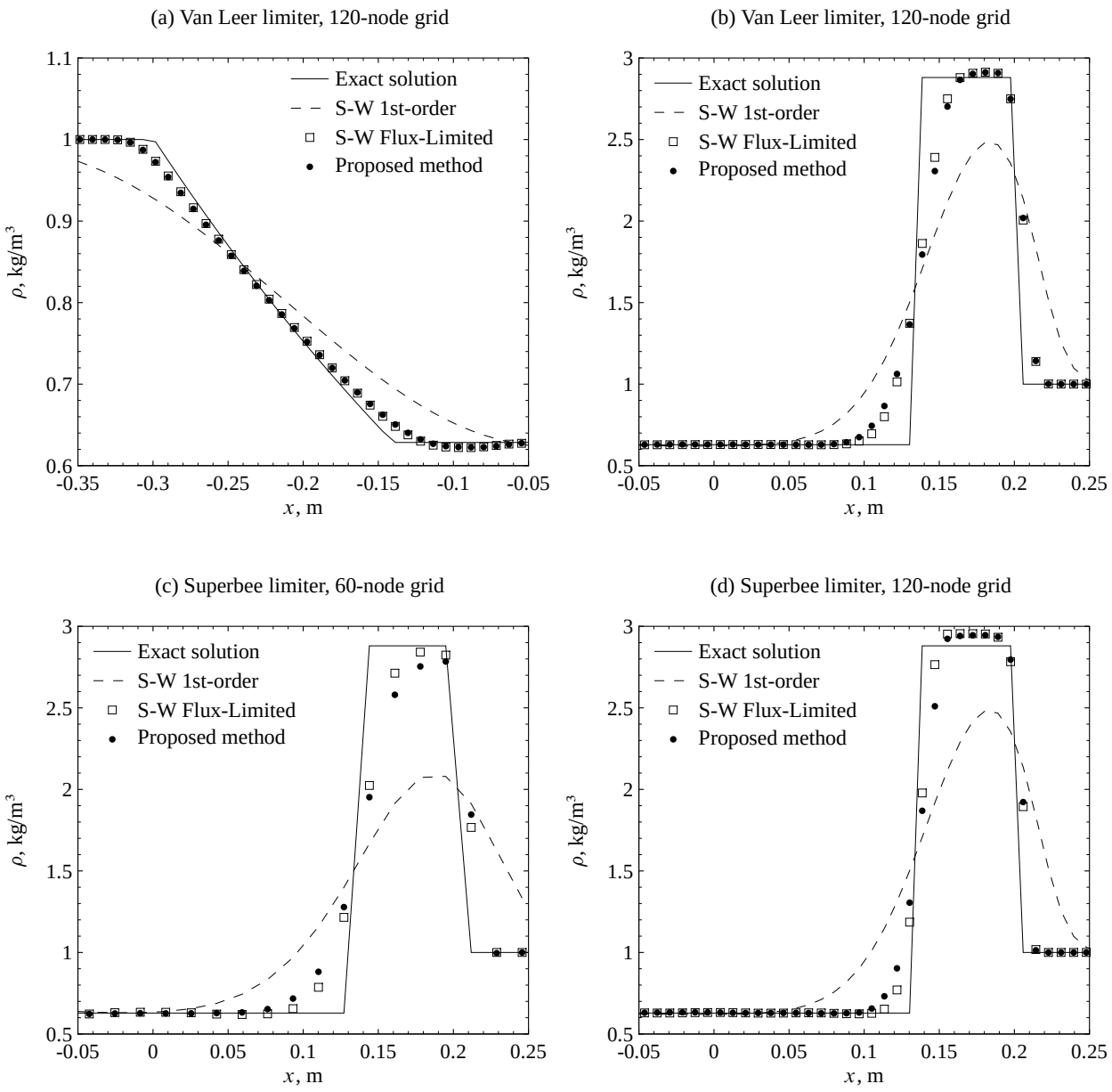

FIGURE 2. Comparison between the proposed schemes and the conventional flux-limited methods on the basis of density profiles for test case #1. The density profiles are obtained at $t = 0.8$ ms using a time step size such that the maximum Courant number within the domain is 0.1.

densities are sometimes obtained.

What makes the discretization stencils outlined herein particularly appealing is their capability to be positivity-preserving while being high-resolution for all wave types. This is not the case for previous flux-limited positivity-preserving second-order accurate methods. For instance, in Ref. [11], a positivity-preserving flux-limited method (denoted as POSFL) is presented and is shown to be second-order accurate. However, POSFL is not high-resolution in the vicinity of contact surfaces where it introduces excessive dissipation compared to the conventional TVD schemes. This was attributed to POSFL forcing the limiter function to be the same over all flux components. But such is not the case for the stencils proposed herein, which allow the limiter function to have a different value for each flux component (i.e. component-wise flux limiting). As shown in Fig. 1, the proposed schemes exhibit considerably higher resolution than POSFL in the vicinity of the contact surface, either when using the minmod limiter or when using the superbee limiter. Further, as can be seen from Fig. 2, the difference between the density profiles obtained with the proposed schemes and those obtained with the conventional (non-positivity-preserving) TVD stencils is minimal when solving rarefaction fans, shockwaves, as well as contact discontinuities. This is true irrespectively of

TABLE 3.
Assessment of relative error of various schemes when solving some 1D test cases.[a,b,c,d]

	Relative error on density, $\frac{1}{\rho_{\text{ref}} L}\int_{-L/2}^{L/2} \lvert\rho - \rho_{\text{exact}}\rvert \, \mathrm{d}x$							
	100-node grid				1000-node grid			
Method	Case #1	Case #2	Case #5	Case #7	Case #1	Case #2	Case #5	Case #7
Steger-Warming (first-order)	12.08%	14.25%	10.70%	3.99%	3.06%	7.06%	1.10%	1.03%
S-W flux limited (Van Leer)	4.62%	-	5.53%	1.07%	0.66%	-	0.64%	0.21%
S-W MUSCL (Van Leer)	3.99%	8.35%	6.99%	0.74%	0.48%	1.50%	0.79%	0.20%
S-W POSFL [11] (Van Leer)	7.74%	13.34%	6.34%	1.53%	1.56%	3.63%	0.69%	0.28%
proposed method (Van Leer)	5.14%	10.54%	7.24%	1.07%	0.74%	2.12%	0.79%	0.21%

[a] The time step is constant for all nodes and is such that the maximum Courant number within the domain is 0.1
[b] The length of the problem L is fixed to 1 m.
[c] The reference density ρ_{ref} is fixed to $\max(\rho_{\text{L}},\ \rho_{\text{R}})$ with ρ_{L} and ρ_{R} being the initial left and right states densities.
[d] The relative error is measured at $t = 0.8$ ms, $t = 0.11$ ms, $t = 0.3$ ms, and $t = 1$ ms for cases #1, #2, #5, and #7 respectively.

TABLE 4.
List of 2D and 3D test cases and initial conditions.

		Left initial state ($x \leq 0$)					Right initial state ($x > 0$)				
Case	Description	T, K	M_x	M_y	M_z	P, bar	T, K	M_x	M_y	M_z	P, bar
#8	2D enclosure[a]	35	10	-3		0.1	35	10	2		0.1
#9	2D Mach 20 external flow[b]	30	16.38	11.47		0.1	30	16.38	11.47		0.1
#10	3D enclosure[c]	300	-40	20	20	0.1	300	40	-20	-20	0.1
#11	2D channel with wavy-wall[d]	300	3	0		0.102	300	3	0		0.102

[a] The flow is enclosed within $-1 \leq x \leq 1$ m and $0 \leq y \leq 1$ m, with a cutout located within $-0.52 \leq x \leq 0$ m and $0 \leq y \leq 0.24$ m. The grid spacing is fixed to $(1/50)$ m along both dimensions.
[b] The flow is enclosed within $0 \leq x \leq 1$ m and $0 \leq y \leq 1$ m, with a cutout located within $(74/300) \leq x \leq (225/300)$ m and $(124/300) \leq y \leq (175/300)$ m. The grid spacing is fixed to $(1/300)$ m along both dimensions.
[c] The flow is enclosed within $-0.5 \leq x \leq 0.5$ m and $0 \leq y \leq 1$ m and $0 \leq z \leq 1$ m, with a cutout located within $-(27/158) \leq x \leq (27/158)$ m and $0 \leq y \leq (53/79)$ m and $0 \leq z \leq (53/79)$ m. The grid spacing is fixed to $(1/79)$ m along the three dimensions.
[d] The channel starts at $x = 0$ and ends at $x = 2$ m, with the top wall located at $y = 0.5$ m and the bottom wall located at $y = \frac{1}{50}\sin(3\pi x)$ m. The grid is composed of 100×25 nodes (uniformly spaced).

the limiter used. The high-resolution capability of the proposed method is further confirmed in Table 3 in which the relative error on the density is tabulated for various test cases and meshes. While a small amount of dissipation is introduced in order to guarantee positivity-preservation, such is generally minimal and does not affect appreciably the resolution in the vicinity of contact surfaces, shocks, or within expansion fans.

6.2. Two- and Three-Dimensional Euler Flow

Although the method is derived in 1D, it can be applied to 2D and 3D problems by discretizing each derivative through 1D operators. For instance, when solving the 2D or 3D Euler equations in generalized curvilinear coordinates:

$$\frac{\partial U}{\partial t} + \sum_{i=1}^{d} \frac{\partial F_i}{\partial X_i} = 0 \tag{60}$$

TABLE 5.
Assessment of positivity-preserving capability of various schemes when solving the 2D and 3D test cases.

	Positivity Preserving?											
	CFL=0.01[a]			CFL=0.166[a]			CFL=0.25[a]			CFL=0.5[a]		
Method	Case #8	#9	#10	Case #8	#9	#10	Case #8	#9	#10	Case #8	#9	#10
Roe (first-order)	Yes	Yes	No	Yes	Yes	No	No	Yes	No	No	Yes	No
Steger-Warming (first-order)	Yes	Yes	Yes	Yes	Yes	Yes	Yes	Yes	Yes	Yes	Yes	No
Yee-Roe (minmod)	No	No	No	No	No	No	No	No	No	No	No	No
S-W flux limited (minmod)	No	No	No	No	No	No	No	No	No	No	No	No
S-W flux limited (Van Leer)	No	No	No	No	No	No	No	No	No	No	No	No
S-W flux limited (superbee)	No	No	No	No	No	No	No	No	No	No	No	No
S-W MUSCL (minmod)	No	No	No	No	No	No	No	No	No	No	No	No
S-W MUSCL (Van Leer)	No	No	No	No	No	No	No	No	No	No	No	No
S-W MUSCL (superbee)	No	No	No	No	No	No	No	No	No	No	No	No
proposed method (minmod)	Yes	Yes	Yes	Yes	Yes	Yes	Yes	Yes	No	No	No	No
proposed method (Van Leer)	Yes	Yes	Yes	Yes	Yes	Yes	Yes	Yes	No	No	No	No
proposed method (superbee)	Yes	Yes	Yes	Yes	Yes	Yes	Yes	Yes	No	No	No	No

[a] The time step is set locally (resulting in a different value for each node) according to Eq. (62).

the time derivative is discretized using a first-order Euler backward stencil and the spatial derivatives are discretized in conservative form as follows:

$$\frac{1}{\Delta t}\left(U^{n+1}-U^{n}\right)+\sum_{i=1}^{d}\left(F_i^{X_i+1/2}-F_i^{X_i-1/2}\right)=0 \tag{61}$$

where the convective flux at the $X_i + 1/2$ interface, $F_i^{X_i+1/2}$, is obtained using the 1D stencils presented in Section 5 [see Eqs. (52)-(57)]. In the latter, d is the number of dimensions, X_i is a generalized coordinate such that the spacing between grid points is 1, and F_i is the convective flux in generalized coordinates (see appendix for a full outline of the Euler equations in generalized curvilinear coordinates).

The solution is advanced in pseudotime using a local time stepping strategy with the local time step set to the minimum CFL condition along all dimensions:

$$\Delta t = \mathrm{CFL}\times\min_{i=1}^{d}\left(\frac{1}{\max_{r}\left|[\Lambda_i]_{r,r}\right|}\right) \tag{62}$$

where CFL is a user-specified constant and Λ_i is the eigenvalue matrix in generalized coordinates (see appendix). For CFL set to 1, it can be easily shown that the latter would yield the largest possible local time step satisfying the CFL condition along each dimension.

Several 2D and 3D test cases are considered, as listed in Table 4. In all cases, the specific heat ratio is fixed to 1.4 and the gas constant is set to 286 J/kg·K. The cases considered are particularly difficult to solve using a discrete method due to the large initial Mach numbers inducing very strong expansion fans within the first few iterations. The zones of low pressure and density created by these strong expansion fans are shown in Figures 3 and 4. Clearly, for test cases #8 and #9 the pressure varies in some areas by 3-6 orders of magnitude within 3-5 grid points. Although not shown here, a similar pressure gradient is observed for test case #10. Due to the presence of these large pressure gradients within few nodes, the numerical methods are prone to yield negative densities and internal energies. Further, because the initial conditions and the problem setups are such that these large pressure gradients are not aligned with the grid lines, these cases serve as an excellent test bed to assess the capabilities of the methods at maintaining positivity-preservation in multidimensional flowfields.

Because the test cases result in flow conditions that are particularly stringent, none of the conventional TVD methods are capable of maintaining the positivity of the density and the internal energy (see Table 5). The lack of success at preserving positivity is not only observed for the flux-limited schemes but is also observed for the MUSCL schemes. While the MUSCL approach combined with the minmod limiter is generally positivity-preserving for 1D flowfields, it is here seen not to be positivity-preserving when used for 2D or 3D problems. The lack of positivity-preservation is not limited to high Courant numbers: lowering the local time step from one quarter to one percent of the minimum CFL condition is observed not to affect

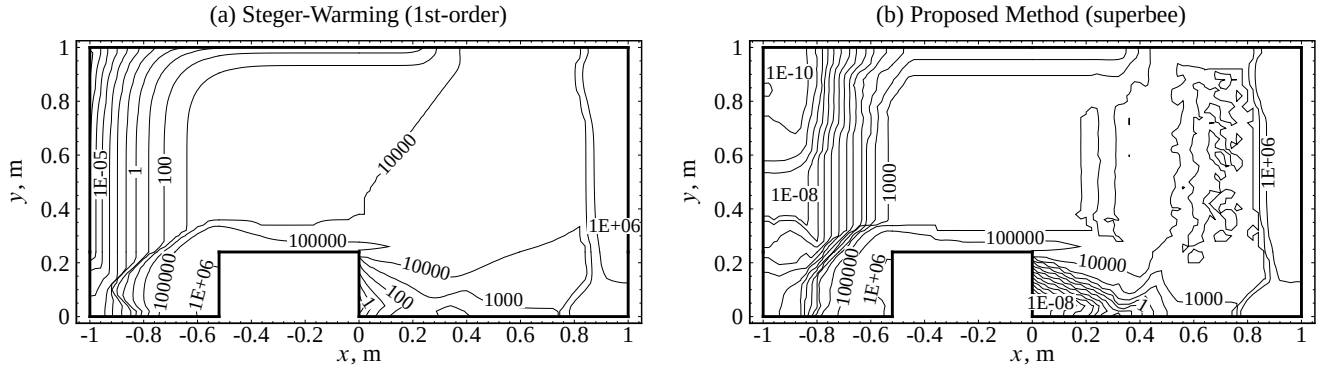

FIGURE 3. Comparison between the first-order Steger-Warming method and the proposed method on the basis of pressure contours (in Pascals) for test case #8 after 100 iterations; the grid spacing is fixed to (1/50) m along both dimensions; the CFL number is fixed to 0.25.

the positivity-preserving capability of the TVD schemes. In fact, only two flux discretization methods are seen to be generally capable to preserve the positivity of the determinative properties at either low or high Courant number: (i) the first-order Steger-Warming method, and (ii) the high-resolution method presented herein.

Interestingly, the Courant number needs to be lowered as the number of dimensions is increased in order to guarantee positivity-preservation. It is recalled that the time step needs to be set to less than half of the CFL condition when solving one-dimensional problems (see proof in Section 4.2). However, when solving multidimensional problems, setting the time step

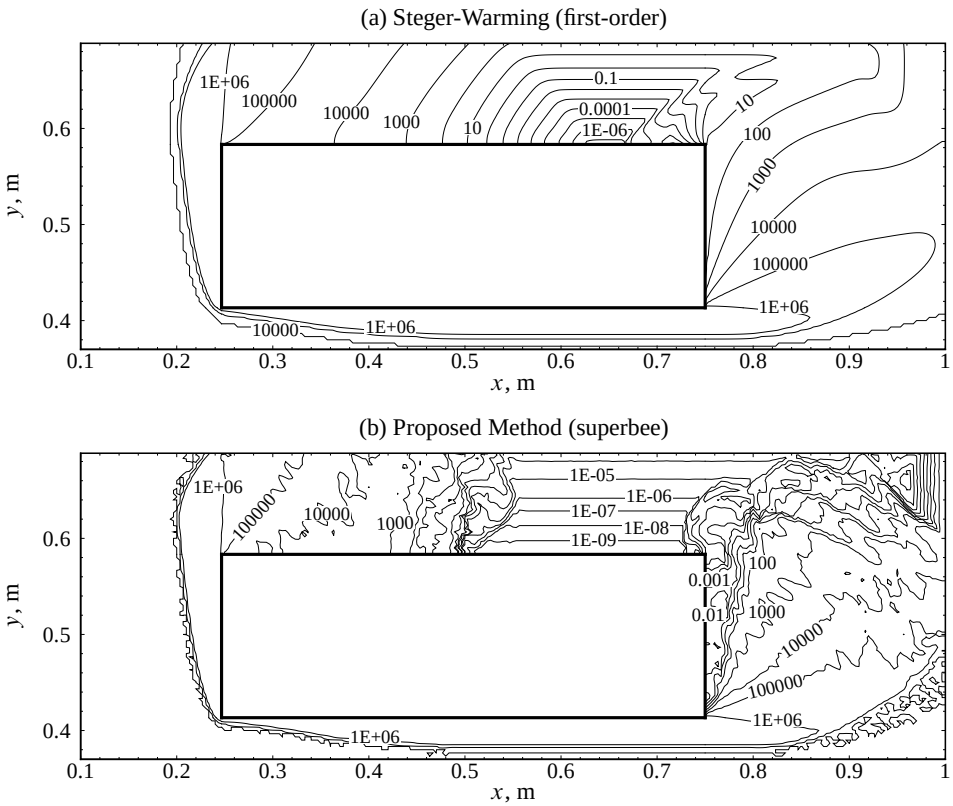

FIGURE 4. Comparison between the first-order Steger-Warming method and the proposed method on the basis of pressure contours (in Pascals) for test case #9 after 300 iterations; the grid spacing is fixed to (1/300) m along both dimensions; the CFL number is fixed to 0.25.

in this manner would sometimes result in negative densities or internal energies. Through trial and error, it is found that the CFL number must be set to no more than $1/4$ and $1/6$ in 2D and 3D respectively to guarantee positivity-preservation (see results in Table 5). Such a necessary reduction of the time step for higher number of dimensions is not specific to the proposed stencils. In fact, a similar trend can be observed for the first-order Steger-Warming method: as the number of dimensions is increased, the CFL number needs to be lowered to ensure that the determinative properties remain positive.

Because the schemes outlined herein achieve positivity-preservation by limiting the second-order terms more substantially than the standard TVD stencils, it may be argued that positivity-preservation is achieved at the expense of resolution. But such a loss in resolution is verified not to be substantial. Indeed, as would be expected from a second-order stencil, the proposed method results in a much improved resolution of shockwaves and especially of expansion fans when compared to the first-order Steger-Warming method (see Figs. 3 and 4). Further, whenever it was possible to compare the results obtained with the proposed schemes to those obtained with the conventional flux-limited methods (that is, when the conventional methods did not yield negative internal energy or density), negligible differences were observed. This is well illustrated in Fig. 5, where steady-state

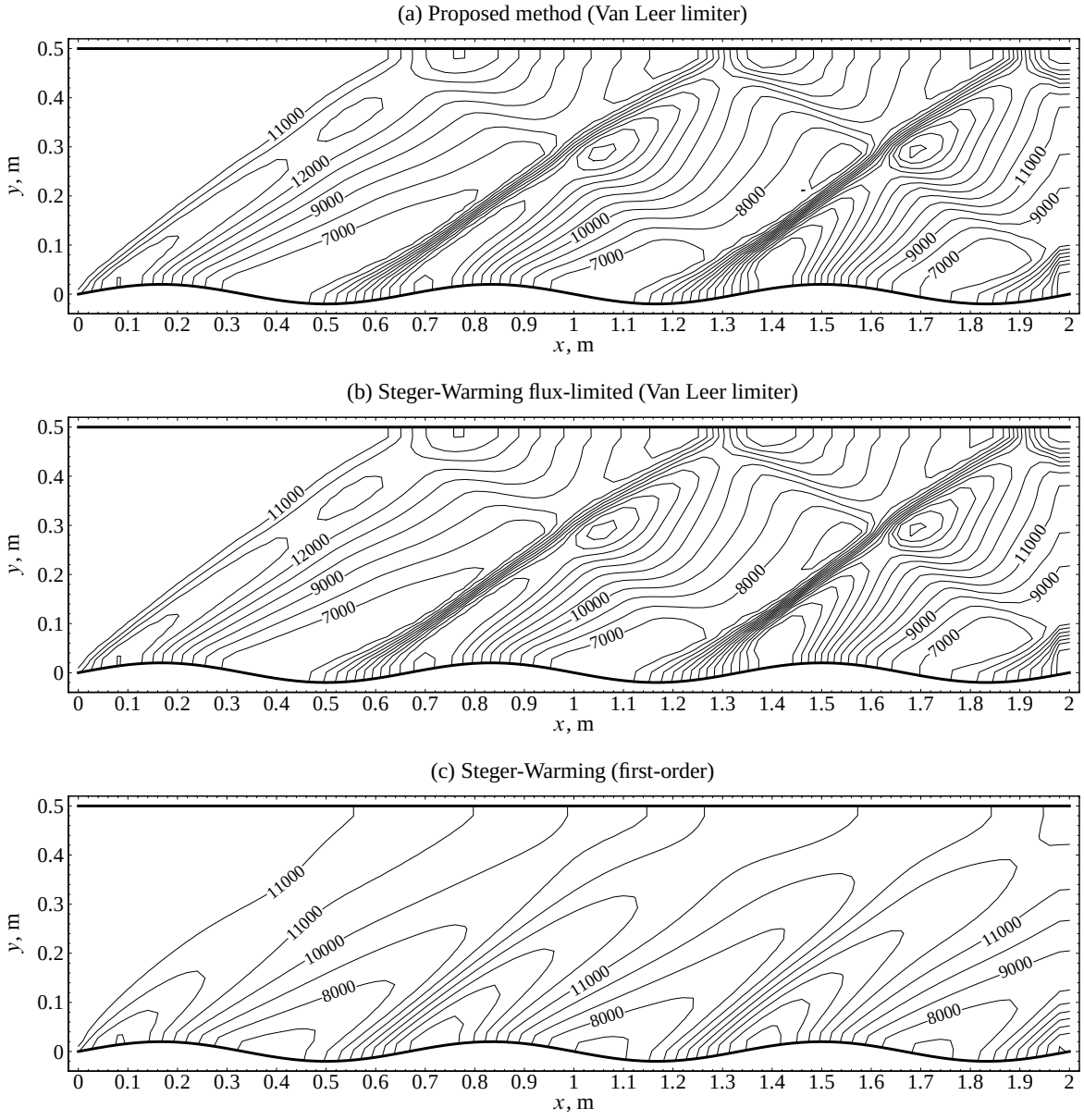

FIGURE 5. Comparison between the proposed method, the conventional TVD scheme, and the first-order Steger-Warming scheme on the basis of steady-state pressure contours (in Pascals) for test case #11.

results of a Mach 3 flow in a wavy-wall channel are depicted. Clearly, there is little to no discernible difference between the pressure contours obtained with both approaches. Although not shown here, results obtained for various other test cases confirm that the extra amount of dissipation necessary for positivity-preservation is typically negligible, and only becomes significant when the conventional TVD schemes introduce negative internal energies or densities.

7. Conclusions

A new class of flux-limited schemes is proposed for systems of conservation laws that is both positivity-preserving and high-resolution. The schemes achieve high-resolution by extending the Steger-Warming method to second-order accuracy through the use of component-wise TVD flux limiters and achieve positivity-preservation by reducing the limiter function such that the discretization equation satisfies the rule of the positive coefficients.

In ensuring that the discretization equation satisfies the rule of the positive coefficients, it is found that the time step is restricted by a CFL-like condition. Specifically, for high-resolution discretizations of 1D systems of conservation laws, it is shown analytically that the time step can not exceed half of the one obtained through the CFL condition in order to guarantee positivity-preservation. For 2D and 3D systems of conservation laws, it is found empirically that the solution remains positivity-preserving as long as the time step does not exceed one quarter and one sixth of the CFL condition, respectively.

Several test cases are considered to assess the positivity-preserving capability of the proposed schemes. The test cases consist of the solution of the 1D Euler equations in Cartesian coordinates and of the solution of the 2D and 3D Euler equations in generalized curvilinear coordinates. Because of the particularly stringent flow conditions encountered through these test cases (e.g. vacuum generation, strong rarefaction fans with the density varying by 3-6 orders of magnitude within a few grid points, Mach 20 flow emanating from a corner, etc), all of the conventional TVD methods fail to preserve positivity of the density or of the internal energy for at least one test case. In fact, only two methods are observed to be generally positivity-preserving: (i) the first-order Steger-Warming scheme, and (ii) the high-resolution schemes presented in this paper.

Because the discretization stencils presented herein achieve positivity-preservation by reducing the limiter function, they are more dissipative than the conventional TVD methods. However, it is found that the additional dissipation needed for positivity-preservation is typically negligible. In fact, when comparing properties obtained with the proposed schemes to those obtained with the conventional TVD methods for several test cases (including time-accurate shock-tube problems and steady-state multidimensional problems), the differences are found to be minimal and barely discernible except when the flow conditions are such that the conventional methods yield negative internal energies or densities. Even then, the loss of resolution is small and the solution obtained remains second-order accurate.

By allowing the flux limiter to have a different value for each flux component (component-wise flux limiting), the method outlined herein can capture with high resolution contact discontinuities as well as shocks and expansion fans. This is in contrast to previous positivity-preserving flux-limited schemes which introduced excessive dissipation in the vicinity of contact surfaces by forcing the limiter to be a constant over all flux components.

Due to being written in general matrix form, the proposed stencils can be used without modification to discretize the fluxes of any system of conservation laws as long as the equations are homogeneous of degree one. Positivity-preservation is guaranteed if the system of conservation laws satisfies the rule of the positive coefficients, as is the case for the Euler equations. To satisfy the rule of the positive coefficients, the system of conservation laws must be such that the determinative properties remain positive when the coefficients of the discretization equation have all-positive eigenvalues and have the same eigenvectors as those of the convective flux Jacobian evaluated at the corresponding node.

Acknowledgment

This work was supported for two years by a Pusan National University Research Grant.

A. Euler Equations and Recommended Eigenvectors

The set of eigenvectors associated with the Euler equations is not unique (in fact, in 2D or 3D, there exists an infinity of different sets). Because the chosen set of eigenvectors can (i) affect the positivity-preserving capability of the method and (ii) affect the resolution of the method, it is necessary to implement the eigenvectors as outlined below in order to reproduce exactly the results shown in this paper.

A.1. One-Dimensional Euler Equations in Cartesian Coordinates

The time-dependent 1D Euler equations can be written in Cartesian coordinates as follows:

$$\frac{\partial U}{\partial t} + \frac{\partial F}{\partial x} = 0 \tag{A.1}$$

The conserved variables vector U, convective flux vector F, eigenvalue matrix Λ, right eigenvector matrix L^{-1}, and characteristic variables vector LU are set to:

$$U = \left[\begin{array}{ccc} \rho & \rho u & \frac{1}{\gamma(\gamma-1)}\rho a^2 + \frac{1}{2}\rho u^2 \end{array} \right]^{\mathrm{T}} \tag{A.2}$$

$$F = \left[\begin{array}{ccc} \rho u & \rho u^2 + \frac{1}{\gamma}\rho a^2 & \frac{1}{\gamma-1}\rho u a^2 + \frac{1}{2}\rho u^3 \end{array} \right]^{\mathrm{T}} \tag{A.3}$$

$$\Lambda = \left[\begin{array}{ccc} u & u+a & u-a \end{array} \right]^{\mathrm{D}} \tag{A.4}$$

$$L^{-1} = \left[\begin{array}{ccc} 1 & u & \frac{1}{2}u^2 \\ 1 & u+a & \frac{1}{\gamma-1}a^2 + \frac{1}{2}u^2 + au \\ 1 & u-a & \frac{1}{\gamma-1}a^2 + \frac{1}{2}u^2 - au \end{array} \right]^{\mathrm{T}} \tag{A.5}$$

$$LU = \left[\begin{array}{ccc} \frac{\gamma-1}{\gamma}\rho & \frac{1}{2\gamma}\rho & \frac{1}{2\gamma}\rho \end{array} \right]^{\mathrm{T}} \tag{A.6}$$

A.2. Multidimensional Euler Equations in Generalized Curvilinear Coordinates

The two-dimensional and three-dimensional Euler equations can be written in generalized curvilinear coordinates as follows:

$$\frac{\partial U}{\partial t} + \sum_{i=1}^{d} \frac{\partial F_i}{\partial X_i} = 0 \tag{A.7}$$

where the convective flux vector has the following property:

$$F_i = A_i U = L_i^{-1} \Lambda_i L_i U \tag{A.8}$$

In the latter, d is the number of dimensions, U is the vector of conserved variables, X is a generalized coordinate such that the spacing between adjacent grid points is 1, A_i is the convective flux Jacobian (i.e. $A_i = \partial F_i / \partial U$), Λ_i is the eigenvalue matrix, and L_i^{-1} is the right eigenvector matrix.

The conserved variables vector U, convective flux vector F, eigenvalue matrix Λ, right eigenvector matrix L^{-1}, and characteristic variables vector LU are set in 2D to:

$$U = J^{-1} \times \left[\begin{array}{ccc} \rho & \rho u & \rho v & \frac{1}{\gamma(\gamma-1)}\rho a^2 + \frac{1}{2}\rho q^2 \end{array} \right]^{\mathrm{T}} \tag{A.9}$$

$$F_i = J^{-1} \times \left[\begin{array}{ccc} \rho V_i & \rho u V_i + \frac{1}{\gamma}\rho a^2 X_{i,1} & \rho v V_i + \frac{1}{\gamma}\rho a^2 X_{i,2} & \frac{1}{\gamma-1}\rho a^2 V_i + \frac{1}{2}\rho q^2 V_i \end{array} \right]^{\mathrm{T}} \tag{A.10}$$

$$\Lambda_i = \left[\begin{array}{ccc} V_i & V_i & V_i + a\left(X_{i,1}^2 + X_{i,2}^2\right)^{\frac{1}{2}} \quad V_i - a\left(X_{i,1}^2 + X_{i,2}^2\right)^{\frac{1}{2}} \end{array} \right]^{\mathrm{D}} \tag{A.11}$$

$$L_i^{-1} = \left[\begin{array}{cccc} 1 & u + a\widehat{X}_{i,2} & v - a\widehat{X}_{i,1} & \frac{1}{2}q^2 + a\left(u\widehat{X}_{i,2} - v\widehat{X}_{i,1}\right) \\ 1 & u - a\widehat{X}_{i,2} & v + a\widehat{X}_{i,1} & \frac{1}{2}q^2 + a\left(v\widehat{X}_{i,1} - u\widehat{X}_{i,2}\right) \\ 1 & u + a\widehat{X}_{i,1} & v + a\widehat{X}_{i,2} & \frac{1}{\gamma-1}a^2 + \frac{1}{2}q^2 + a\left(u\widehat{X}_{i,1} + v\widehat{X}_{i,2}\right) \\ 1 & u - a\widehat{X}_{i,1} & v - a\widehat{X}_{i,2} & \frac{1}{\gamma-1}a^2 + \frac{1}{2}q^2 - a\left(u\widehat{X}_{i,1} + v\widehat{X}_{i,2}\right) \end{array} \right]^{\mathrm{T}} \tag{A.12}$$

$$L_i U = \left[\begin{array}{cccc} \frac{\gamma-1}{2\gamma}\rho & \frac{\gamma-1}{2\gamma}\rho & \frac{1}{2\gamma}\rho & \frac{1}{2\gamma}\rho \end{array} \right]^{\mathrm{T}} \tag{A.13}$$

and in 3D to:

$$U = J^{-1} \times \left[\begin{array}{cccc} \rho & \rho u & \rho v & \rho w & \frac{1}{\gamma(\gamma-1)}\rho a^2 + \frac{1}{2}\rho q^2 \end{array} \right]^{\mathrm{T}} \tag{A.14}$$

$$F_i = J^{-1} \times \left[\begin{array}{cccc} \rho V_i & \rho u V_i + \frac{1}{\gamma}\rho a^2 X_{i,1} & \rho v V_i + \frac{1}{\gamma}\rho a^2 X_{i,2} & \rho w V_i + \frac{1}{\gamma}\rho a^2 X_{i,3} & \frac{1}{\gamma-1}\rho a^2 V_i + \frac{1}{2}\rho q^2 V_i \end{array} \right]^{\mathrm{T}} \tag{A.15}$$

$$\Lambda_i = \left[\begin{array}{ccccc} V_i & V_i & V_i & V_i + a\left(X_{i,1}^2 + X_{i,2}^2 + X_{i,3}^2\right)^{\frac{1}{2}} & V_i - a\left(X_{i,1}^2 + X_{i,2}^2 + X_{i,3}^2\right)^{\frac{1}{2}} \end{array} \right]^{\mathrm{D}} \tag{A.16}$$

$$L_i^{-1} = \left[\begin{array}{ccccc} 1 & u + a\left(\widehat{X}_{i,2} + \widehat{X}_{i,3}\right) & v - a\widehat{X}_{i,1} & w - a\widehat{X}_{i,1} & \frac{1}{2}q^2 + au\left(\widehat{X}_{i,2} + \widehat{X}_{i,3}\right) - a\left(v + w\right)\widehat{X}_{i,1} \\ 1 & u - a\widehat{X}_{i,2} & v + a\left(\widehat{X}_{i,1} + \widehat{X}_{i,3}\right) & w - a\widehat{X}_{i,2} & \frac{1}{2}q^2 + av\left(\widehat{X}_{i,1} + \widehat{X}_{i,3}\right) - a\left(u + w\right)\widehat{X}_{i,2} \\ 1 & u - a\widehat{X}_{i,3} & v - a\widehat{X}_{i,3} & w + a\left(\widehat{X}_{i,1} + \widehat{X}_{i,2}\right) & \frac{1}{2}q^2 + aw\left(\widehat{X}_{i,1} + \widehat{X}_{i,2}\right) - a\left(u + v\right)\widehat{X}_{i,3} \\ 1 & u + a\widehat{X}_{i,1} & v + a\widehat{X}_{i,2} & w + a\widehat{X}_{i,3} & \frac{1}{\gamma - 1}a^2 + \frac{1}{2}q^2 + a\left(u\widehat{X}_{i,1} + v\widehat{X}_{i,2} + w\widehat{X}_{i,3}\right) \\ 1 & u - a\widehat{X}_{i,1} & v - a\widehat{X}_{i,2} & w - a\widehat{X}_{i,3} & \frac{1}{\gamma - 1}a^2 + \frac{1}{2}q^2 - a\left(u\widehat{X}_{i,1} + v\widehat{X}_{i,2} + w\widehat{X}_{i,3}\right) \end{array} \right]^{\mathrm{T}} \tag{A.17}$$

$$L_i U = \left[\begin{array}{ccccc} \frac{\gamma - 1}{3\gamma}\rho & \frac{\gamma - 1}{3\gamma}\rho & \frac{\gamma - 1}{3\gamma}\rho & \frac{1}{2\gamma}\rho & \frac{1}{2\gamma}\rho \end{array} \right]^{\mathrm{T}} \tag{A.18}$$

In the latter, the flow speed, the contravariant velocity, the inverse of the metric Jacobian, the spatial derivative of the generalized coordinate, and the normalized spatial derivative of the generalized coordinate correspond to:

$$q^2 = u^2 + v^2 + w^2 \tag{A.19}$$

$$V_i = uX_{i,1} + vX_{i,2} + wX_{i,3} \tag{A.20}$$

$$\frac{1}{J} = \begin{cases} \dfrac{\partial x_1}{\partial X_1}\dfrac{\partial x_2}{\partial X_2} - \dfrac{\partial x_1}{\partial X_2}\dfrac{\partial x_2}{\partial X_1} & \text{in 2D} \\ \displaystyle\sum_{i=1}^{3}\left(\frac{\partial x_1}{\partial X_i}\frac{\partial x_2}{\partial X_{i+1}}\frac{\partial x_3}{\partial X_{i+2}} - \frac{\partial x_1}{\partial X_i}\frac{\partial x_2}{\partial X_{i+2}}\frac{\partial x_3}{\partial X_{i+1}}\right) & \text{in 3D} \end{cases} \tag{A.21}$$

$$X_{i,j} = \frac{\partial X_i}{\partial x_j} = \begin{cases} J\left(\left(2\delta_{ij} - 1\right)\dfrac{\partial x_{j+1}}{\partial X_{i+1}}\right) & \text{in 2D} \\ J\left(\dfrac{\partial x_{j+1}}{\partial X_{i+1}}\dfrac{\partial x_{j+2}}{\partial X_{i+2}} - \dfrac{\partial x_{j+2}}{\partial X_{i+1}}\dfrac{\partial x_{j+1}}{\partial X_{i+2}}\right) & \text{in 3D} \end{cases} \tag{A.22}$$

$$\widehat{X}_{i,j} = X_{i,j} \Bigg/ \left(\sum_{j=1}^{d} X_{i,j}^2\right)^{\frac{1}{2}} \tag{A.23}$$

where δ_{ij} is the Kronecker delta and where a cyclic permutation of the indices is implied (with the minimum and maximum being 1 and d respectively).

References

[1] FAZIO, R. AND JANNELLI, A., "Second Order Positive Schemes by means of Flux Limiters for the Advection Equation," *IAENG International Journal of Applied Mathematics*, Vol. 39, No. 1, 2009, pp. 4.

[2] MACKINNON, R. J. AND CAREY, G. F., "Positivity-Preserving, Flux-limited Finite-difference and Finite-element Methods for Reactive Transport," *International Journal for Numerical Methods in Fluids*, Vol. 41, 2003, pp. 151–183.

[3] EINFELDT, B., MUNZ, C. D., ROE, P. L., AND SJOGREEN, B., "On Godunov-type Methods near Low Densities," *Journal of Computational Physics*, Vol. 92, 1991, pp. 273–295.

[4] GRESSIER, J., VILLEDIEU, P., AND MOSCHETTA, J.-M., "Positivity of Flux Vector Splitting Schemes," *Journal of Computational Physics*, Vol. 155, No. 1, 1999, pp. 199–220.

[5] PERTHAME, B. AND SHU, C.-W., "On Positivity-Preserving Finite Volume Schemes for Euler Equations," *Numerische Mathematik*, Vol. 73, 1996, pp. 119–130.

[6] BERTHON, C., "Stability of the MUSCL Schemes for the Euler Equations," *Communications in Mathematical Sciences*, Vol. 3, No. 2, 2005, pp. 133–157.

[7] BERTHON, C., "Robustness of MUSCL Schemes for 2D Unstructured Meshes," *Journal of Computational Physics*, Vol. 218, 2006, pp. 495–509.

[8] WAAGAN, K., "A Positive MUSCL-Hancock Scheme for Ideal Magnetohydrodynamics," *Journal of Computational Physics*, Vol. 228, 2009, pp. 8609–8626.

[9] WANG, C. AND LIU, J.-G., "Positivity Property of Second-Order Flux-Splitting Schemes for the Compressible Euler Equations," *Discrete and Continuous Dynamical Systems – Series B*, Vol. 3, No. 2, May 2003, pp. 201–228.

[10] FRIEDRICHS, K. O., "Symmetric Hyperbolic Linear Differential Equations," *Communications on Pure and Applied Mathematics*, Vol. 7, No. 2, 1954, pp. 345–392.

[11] PARENT, B., "Positivity-Preserving Flux-Limited Method for Compressible Fluid Flow," *Computers & Fluids*, Vol. 44, 2011, pp. 238–247.

[12] STEGER, J. L. AND WARMING, R. F., "Flux Vector Splitting of the Inviscid Gasdynamics Equations with Application to Finite Difference Methods," *Journal of Computational Physics*, Vol. 40, 1981, pp. 263–293.

[13] LANEY, C. B., *Computational Gasdynamics*, Cambridge University Press, Cambridge, New-York, NY, 1998.

[14] VAN LEER, B., "Towards the Ultimate Conservation Scheme II. Monotonicity and Conservation Combined in a Second-Order Scheme," *Journal of Computational Physics*, Vol. 14, 1974, pp. 361–370.

[15] ROE, P., "Characteristic-based Schemes for the Euler Equations," *Annual Review of Fluid Mechanics*, Vol. 18, 1986, pp. 337.

[16] ROE, P. L., "Approximate Riemann Solvers, Parameter Vectors, and Difference Schemes," *Journal of Computational Physics*, Vol. 43, 1981, pp. 357–372.

[17] YEE, H. C., KLOPFER, G. H., AND MONTAGNÉ, J.-L., "High-Resolution Shock-Capturing Schemes for Inviscid and Viscous Hypersonic Flows," *Journal of Computational Physics*, Vol. 88, 1990, pp. 31–61.

[18] ANDERSON, W. K., THOMAS, J. L., AND VAN LEER, B., "Comparison of Finite Volume Flux Volume Flux Vector Splittings for the Euler Equations," *AIAA Journal*, Vol. 24, 1986, pp. 1453–1460.